

Supplementary information related to experiments is specific to the NIPAAm-based BZ gels discussed in the main text.

A. Experimental details and discussion

To quantify the oxidation state of the Ru(bpy)₃ catalyst, the red (*R*), green (*G*), and blue (*B*) values for each point of analysis were recorded in order to calculate the hue, as defined on cylindrical coordinates.^[1] The following equations were used to determine hue, in degrees:

$$\alpha = R - 0.5(G + B) \quad (1)$$

$$\beta = \frac{\sqrt{3}}{2}(G - B) \quad (2)$$

$$\text{Hue} = \frac{180}{\pi} \text{atan2}(\beta, \alpha) \quad (3)$$

The period of oscillation was quantified by calculating the elapsed time between peaks of hue corresponding to oxidized ruthenium, as shown in Figure S1. For patterned gels, the period was quantified for late time patterns. The wave velocity was extracted by analyzing two points of interest along which the BZ waves travel (separated by a distance *x*).

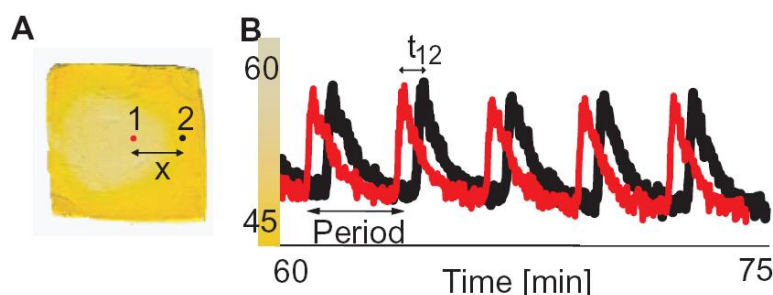


Figure S1. Quantification of oscillation characteristics. (A) Representative points of interest in a patterned gel of lateral dimensions 3.3 x 3.3 mm. (B) Wave velocity v is determined as $v=x/t_{12}$, and period is the time between amplitude maxima at a given point.

A summary of the oscillation period and wave velocity of rectangular gels at late reaction times is given in Table S1. The oscillation period at late reaction times (i.e., at least 30 min after the reaction was initiated) is quantified in comparison to the period observed at early reaction times (i.e., less than 30 min after the reaction was initiated). Note that gels of aspect ratio ~ 4 and volume $\sim 90\text{mm}^3$ exhibit oscillation periods of ~ 2 min at both early and late times, agreeing well with that observed in gels of aspect ratio 1 and 2 and with simulation predictions. However, gels of aspect ratio ~ 4 and volume $\sim 1.4\text{mm}^3$ exhibit oscillation periods of ~ 1 min (early times) and 11 min (late times). This discrepancy between the simulation results and experiments occurs when the absolute dimensions of the gel are sufficiently small.

Table S1. Quantification of oscillations as a function of gel volume and aspect ratio.

Gel volume [mm ³]	Aspect ratio	Early-time Period [min]	Late-time Period [min]	Wave velocity (late-time) [mm/min]
1.4	3.7	1.1 ± 0.2	11.7 ± 0.5	3.6 ± 1.2
4.5	2	1.7 ± 0.2	2.0 ± 0.1	1.7 ± 1.2
14	1	2.2 ± 0.1	2.2 ± 0.1	2.4 ± 0.9
90	4	1.4 ± 0.1	2.1 ± 0.1	2.7 ± 1.0

While Table S1 shows that the period of oscillation is constant over a wide range of gel volumes (4.5-90 mm³), Fig. S2 (inset) shows that the oscillation period increases as the size of the gel decreases for gel volumes less than or equal to 4.5 mm³.

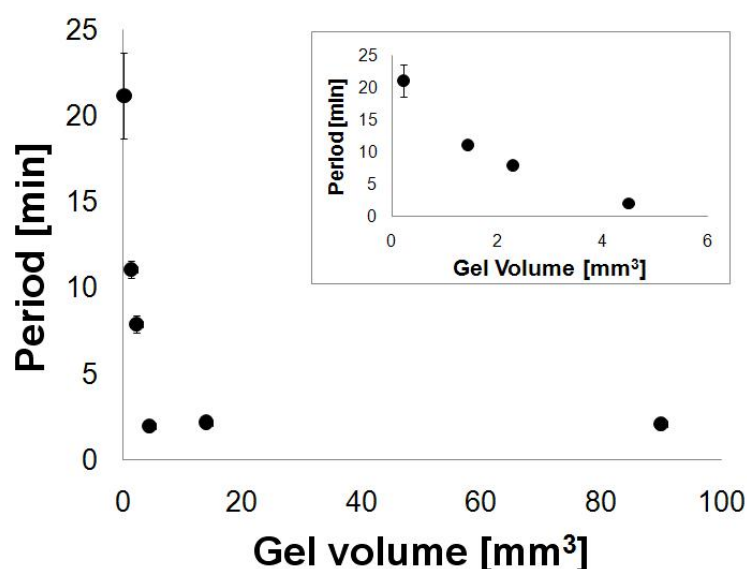


Figure S2. Oscillation period at late-times (i.e., 30 min after oscillations initiated), as a function of gel volume. For gel volumes < 4.5 mm³, oscillation period increases with decreasing gel volume (inset). Error bars represent standard deviation. Note that not all of these gels can be described by a single aspect ratio (e.g., triangular gels) and that not all of these gels transitioned from early- to late-time patterns (e.g., those smaller in one dimension than ~0.6 mm). For this reason, Table S1 comprises only a subset of the experiments shown in this figure.

In addition to quantifying % swelling in small gels of varying Ru(bpy)₃ content (see Figure 4), the amplitude of these oscillations was also quantified according to color change. This hue amplitude was determined by calculating the difference between the maximum hue and the

minimum hue for the first five oscillations for gels synthesized with three different $\text{Ru}(\text{bpy})_3$ concentrations, as shown in Figure S3:

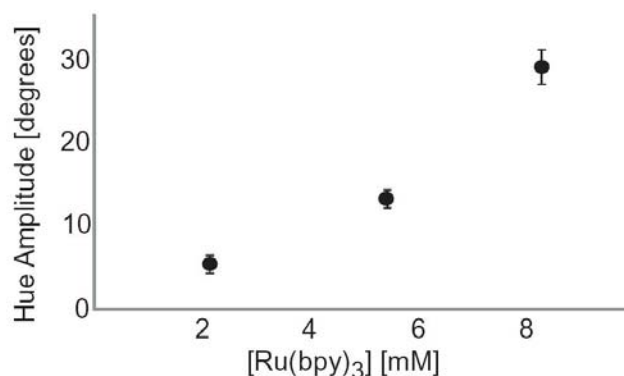


Figure S3. Hue amplitude versus $\text{Ru}(\text{bpy})_3$ concentration. Data shown are average \pm standard deviation among the first five oscillations for each gel. For each sample, gel edges were approximately 0.6 mm.

B. Simulation approach and discussion

The simulation results in Figures 3 and 4 were obtained using the three dimensional gel lattice spring model (3D gLSM) approach developed by us.^[2] To study the effects of the $\text{Ru}(\text{bpy})_3$ content on the behavior of the gels, we modified the reaction kinetics terms (as described below) by utilizing an improved Oregonator model.^[3,4] The values for the majority of the model parameters were based on available experimental data.^[2] To maximize the similarity between the model and the experiments described herein, we adjusted the values of the crosslink density c_0 , the concentration of hydrogen ions H , the Oregonator model parameters ε and f , and the catalyst-solvent interaction parameter χ^* (for details about these parameters see Ref [5].) Specifically, we used the following values: $c_0 = 8 \times 10^{-4}$, $H = 0.9M$, $\varepsilon = 0.025$, $f = 0.9$, and $\chi^* = 0.01$. The parameter χ^* controls the mechanical response of the sample to changes in the concentration of the oxidized catalyst. The value of χ^* was chosen so that the amplitude of the sample's mechanical swelling was similar to that observed in the present experiments. For the above parameter values, the characteristic time and length scales in our simulations were $T_0 \sim 0.33$ s and $L_0 \sim 23 \mu\text{m}$, respectively.

For the cases shown in Figure 3B, we used three different simulation box sizes: $104 \times 104 \times 40$, $97 \times 50 \times 28$, and $94 \times 25 \times 18$ nodes. These dimensions correspond to the sample sizes used in the experiments; namely, with the above scaling, these dimensionless values correspond to the respective dimensional sizes of: $3.3\text{mm} \times 3.3\text{mm} \times 1.3\text{mm}$,

3.1mm × 1.6mm × 0.9mm, and 3.0mm × 0.8mm × 0.6mm. We refer to the later cases as A, B, and C, respectively. In these simulations, the samples are attached only to the bottom substrate; the other faces of the samples are allowed to swell freely in the solvent. (This approximates the state of the immersed gels in the experiments, which rest on a polystyrene Petri dish.) We also note that the color in Figure 3B corresponds to the concentration of the oxidized catalyst according to the color bar provided in Figure 3g of Ref [2]. Here, however, we chose the value of $v_{\max} = 0.22$ (the same color scheme is also used in the Supplementary Information movies of simulations). Namely, in the simulation images in Figure 3B, the blue corresponds to a higher and green corresponds to a lower concentration of oxidized catalyst.

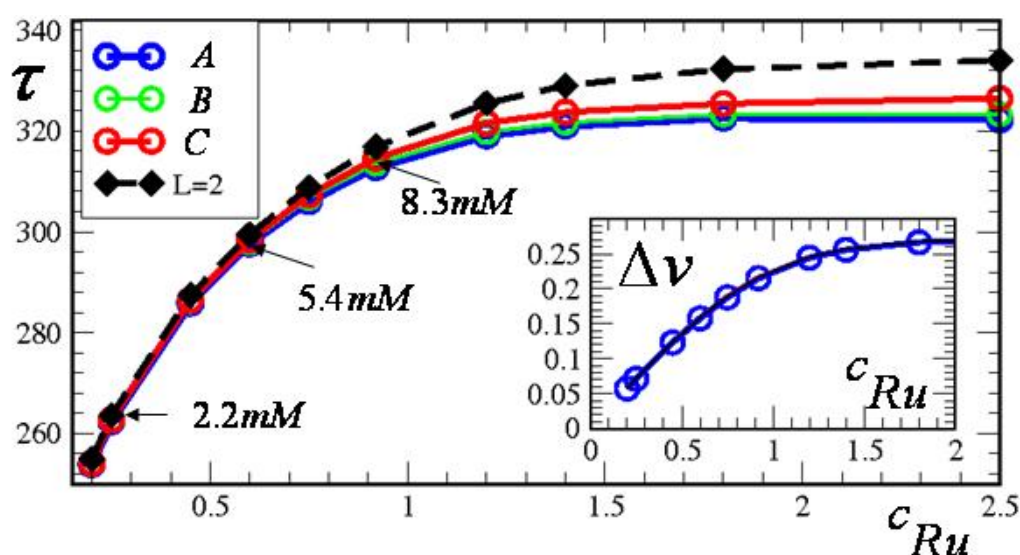


Figure S4. Dependence of the period of oscillations, τ , for all sample sizes (aspect ratios) on the dimensionless total concentration of $\text{Ru}(\text{bpy})_3$ catalyst c_{Ru} . Aspect ratios are given as follows: (A) 1, (B) 2, and (C) 3.7. The points that correspond to the experimental values of $\text{Ru}(\text{bpy})_3$ concentration discussed in the manuscript are marked by the arrows. The inset shows the dependence of the amplitude of oscillations in the concentration of the oxidized catalyst (Δv) on c_{Ru} . Only one line is shown for clarity in the inset because all the lines for samples A-C coincide.

Figure S4 shows the dependence of the period of oscillations on the dimensionless total concentration of $\text{Ru}(\text{bpy})_3$ catalyst, c_{Ru} , for the chosen sample sizes. The solid lines indicate the data for the larger samples (A-C) and the dashed black line marks the results for a smaller, free (unattached) sample that is $2 \times 2 \times 2$ nodes in size. The arrows mark the points that correspond to the experimental values of $\text{Ru}(\text{bpy})_3$ discussed in the paper. The inset

shows how the amplitude of the oscillations in terms of the oxidized catalyst concentration, Δv , depends on c_{Ru} .

As seen in Figure S4, both the period and amplitude of the oscillations of Δv show an increase with increasing total concentration of $Ru(bpy)_3$, and then level off at some plateau values. At the plateau values, the catalyst concentration is sufficiently high that further increases in c_{Ru} do not affect the reaction kinetics. The simulation results also confirm that our original approach to modeling the BZ reaction^[2,5,6] is applicable if the concentration of $Ru(bpy)_3$ content is sufficiently high (i.e., reaches the plateau values); namely, for the chosen set of parameters, our original model is applicable for $[Ru(bpy)_3] > 14$ mM. (The latter value depends on the system parameters; for example, it significantly decreases with decreasing ε .)

The increase in both the period and the amplitude of oscillations of Δv with an increase in $Ru(bpy)_3$ concentration is consistent with the present experimental studies.

Moreover, at higher values of c_{Ru} , the period of oscillations is somewhat higher for the smaller samples (see black dashed line) than for all the larger samples (A-C). It is, however, important to note that the relative increase in the period with an increase in $Ru(bpy)_3$ concentration is significantly smaller in the simulations than in the experiments (hence, this increase is not apparent in Figure 4D where a larger scale is used). This difference could be attributed to the simplicity of the Oregonator model used to describe the reaction kinetics; for example, the model does not account for the depletion of reagents within the sample. Finally, we note that to calculate the simulation points corresponding to the percentage of swelling in Figure 4C, we used all the same parameters as described above, but set the sample size to $2 \times 2 \times 2$ nodes.

Modification of equations for reaction kinetics in gLSM

To account for the effect of the total concentration of $Ru(bpy)_3$ catalyst, we modified our original 3D gLSM approach^[2] by incorporating an improved Oregonator model, which explicitly includes the concentration of the $Ru(bpy)_3$ catalyst, C , in the governing equations.^[3] We utilized this improved model^[3] in a recent study^[4] that provides more detailed discussions of the calculations. Briefly, we replaced the reaction rate terms in Eqs.(5)-(6) of Ref. [2] with the following expressions:^[4]

$$F(u, v, r, \phi) = (1 - \phi)^2 wr - u^2 - (1 - \phi)fv \frac{u - q(1 - \phi)^2}{u + q(1 - \phi)^2}, \quad (4)$$

$$G(u, v, r, \phi) = (1 - \phi)^2 w r - (1 - \phi) v, \quad (5)$$

where

$$w = \mu[r^2 + 2u/\mu]^{1/2} - \mu r, \quad (6)$$

$$r = \xi[c_{Ru}\phi_0^{-1}\phi - v]. \quad (7)$$

In Eq. (7), $c_{Ru} \equiv C/Z_0$ is the dimensionless concentration of Ru(bpy)₃ catalyst, where $Z_0 \approx 9\text{mM}$ (according to the definitions and experimental values in Ref. [5], and taking into account that $H \approx 0.9\text{M}$). The rest of the notation in Eqs. (4)-(7) are the same as in Refs. [2,5]. Herein, we set $\xi = 1$ and $\mu = 90$.^[4]

C. Movies from experiments and simulations

Movies that illustrate self-oscillating experiments in BZ gels are also provided online. These movie files include oscillations as a function of aspect ratio (AR), entitled BZGelExpt_AR1.mpg, BZGelExpt_AR2.mpg, and BZGelExpt_AR4.mpg; video speed is 40x for these 3 files. Additionally, a movie illustrating chemomechanical coupling at sufficiently small dimensions is entitled BZChemomechanical.avi; video speed is 500x. These movies correspond to the still images in Figures 2-4 of the manuscript.

Movies are also supplied to illustrate simulated predictions of the BZ reaction as a function of gel aspect ratio, entitled Simulation_AR1.gif, Simulation_AR2.gif, and Simulation_AR4.gif. These simulations were conducted under comparable absolute gel dimensions and catalyst concentrations to those employed in experiments.

References

- [1] Hanbury, A. *Pattern Recognit. Lett* **29**(4), 494-500 (2008).
- [2] Kuksenok, O., Yashin, V.V., and Balazs, A.C. *Phys. Rev. E* **78**(4), 041406 (2008).
- [3] Amemiya, T., Yamamoto, T., Ohmori, T., and Yamaguchi, T. *J. Phys. Chem. A* **106**(4), 612-620 (2002).
- [4] Yashin, V.V., Kuksenok, O., and Balazs, A.C. *J. Phys. Chem. B* **114**(19), 6316-6322 (2010).
- [5] Yashin, V.V. and Balazs, A.C. *J. Chem. Phys.* **126**(12), 124707 (2007).
- [6] Yashin, V.V. and Balazs, A.C. *Macromolecules* **39**(6), 2024-2026 (2006).